Physical modelling of spectral reflectance

Q. Chen, T.L.V. Cheung, S. Westland
Centre for Colour Design Technology, University of Leeds, United Kingdom
Corresponding author: Q. Chen (texqc@leeds.ac.uk)

ABSTRACT

Linear modelling is a common method to efficiently represent object reflectance spectra. In this paper, an alternative method is used based on the physical characteristics of the spectral reflectance. Because of the band-limited properties of the spectral reflectance and the smoothness of the spectral reflectance curves, we model the reflectance spectra by using modified Gaussian functions to represent absorption properties of the objects, which are physically the primary cause of the spectral reflectance. A set of artificial spectral reflectance generated from this physical model showed very similar characteristics of the Munsell data set, and the reverse of the model can also give accurately reconstruction of the original reflectance spectra.

1. INTRODUCTION

Linear models are frequently used to represent object reflectance spectra[1]. Such models, which usually use principle components or basis functions, have been used for a variety of applications[2] including device characterization and as a basis for possible explanations for colour constancy. Although these linear models are efficient they are derived from the statistical properties of reflectance data sets and consequently the representation of a spectrum in the model does not provide any explicit information about the physical causes of the reflectance spectrum.

The spectral properties of reflectance are primarily determined by the absorption and scattering properties of objects. Nassau noted that the absorption curves of many organic and inorganic substances are composed of superimposed broad bands[3]. Maloney pointed out that the broad, smooth shape of these band spectra determines the smooth shape of spectral reflectance curves[1]. In this work, we attempt to represent object reflectance using a model that is based on the physics of reflectance spectra rather than on their statistical properties. The purpose of such a model is to enable an efficient representation of reflectance spectra that makes the underlying physical processes more explicit.

2. METHOD

We use Gaussian distributions to model the absorbance properties of objects since they closely approximate the physical processes involved in electronic transition absorptions[4]. Each absorption process is represented by three parameters: amplitude, bandwidth and the location of the peak wavelength. The absorption profile of a given object is represented by several overlapping Gaussian distributions. The relationship between absorption and reflectance is known to be non-linear and so the Kubelka-Munk function, $f(P) = (1-P)^2/2P$, is used to relate reflectance P to absorption. The process modelling can be expressed as following equations:

$$P = 1 + K - \sqrt{(1+K)^2 - 1} \tag{1}$$

where P is the reflectance and K is the absorption distribution, and

$$K = K_1 + K_2 + \cdots K_n \tag{2}$$

where K is the total absorption distribution and K_i is the *ith* individual absorption.

$$K_{i\lambda} = a_i \exp\left(-\left(\frac{\lambda - p_i}{w_i}\right)\right)^2 \quad i=1,2...n \qquad \lambda=360,370...780nm \qquad (3)$$

The individual absorption processes are modelled by Equation 3 where $K_{i\lambda}$ is the value of the *ith* absorption at wavelength λ, and a_i, p_i, and w_i represent the amplitude, peak wavelength and half-width (at half-height) of the Gaussian for the *ith* Gaussian absorption distribution respectively.

Figure 1 gives an example of the modelling. In Figure 1(a), three absorption bands are generated (Equation 3) with specified amplitude (0.2, 0.5, 0.8), peak wavelength (330nm, 400nm, 550nm) and half-width (24nm, 50nm, 80nm). Figure 1(b) shows the total absorption distribution calculated by Equation (2) and the Kubelka-Munk function (Equation 1) is applied to generate the reflectance spectrum as presented in Figure 1(c).

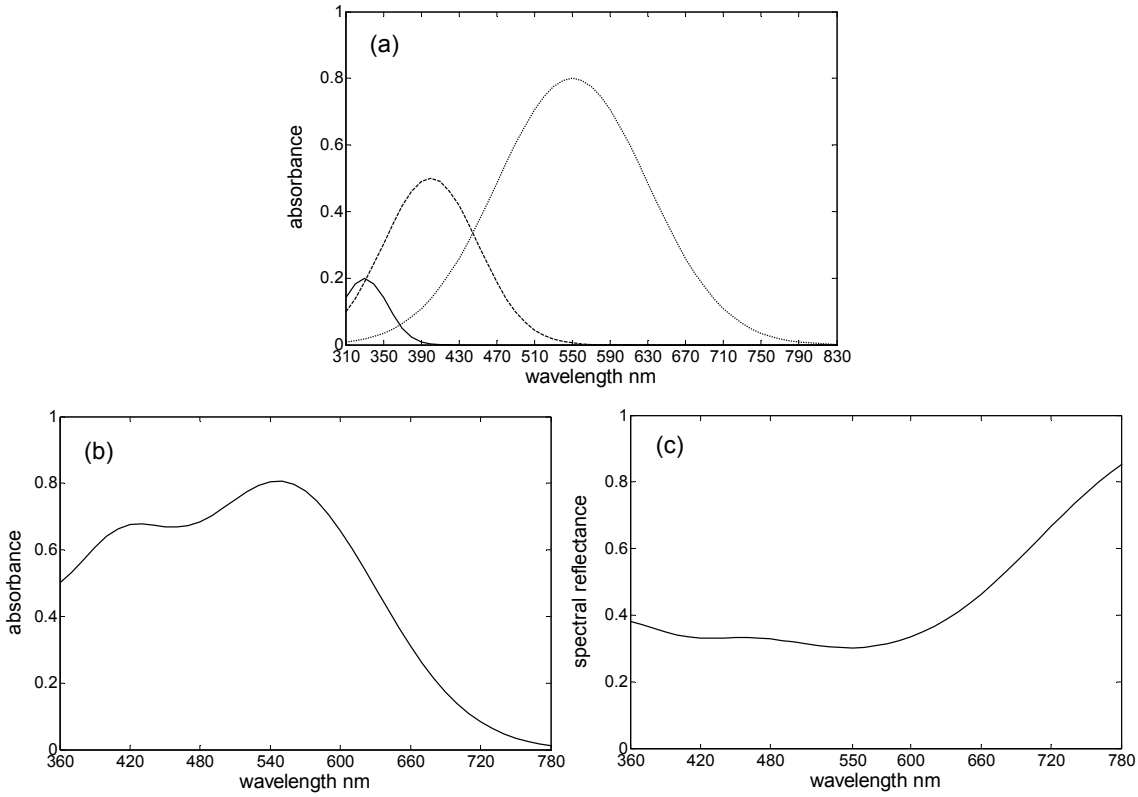

Figure 1: An example of generating reflectance spectra using the physical model showing (a) individual absorption process (first absorption band: solid line; second absorption band: dashed line; third absorption band: dotted line); (b) total absorption profile; (c) final reflectance spectrum.

The model can be used to generate a set of reflectance spectra with physically reasonable properties or an optimization algorithm can be used to find the parameters of the model to best fit any target reflectance spectrum. In this work, a set of 1269 reflectance spectra in the range 360nm to 780nm at intervals of 10nm using the physical model. The number of absorption bands was randomly selected between 1 to 5 and the three parameters of each Gaussian optimized based on initial estimates randomly selected from the range 20nm to 80nm (for the half-width), 310nm to 830nm (for the peak wavelength) and 0-10 (for the amplitude). (The choice of the range for the amplitude allowed the model to generate reflectance values in the approximate range 0.045-1.00.) A set of 100 reflectance spectra from the 1269 Munsell reflectance data set[5] was matched using the physical model. A dynamic hill-climbing optimization procedure[6] was performed to minimize root-mean squared (RMS) error between the target spectra and the matches in the model

3. RESULTS AND CONCLUSIONS

The model generated reflectance spectra in the range of 360nm to 780nm but only the values between 400nm and 700nm were used to compare with the 1269 Musell data set which is in the rang of 400nm and 700nm. Figure 2 shows the chromaticity gamut for both data sets in the CIE *xy* diagram. The gamut of the model reflectances is similar but slightly larger than that of the Munsell data.

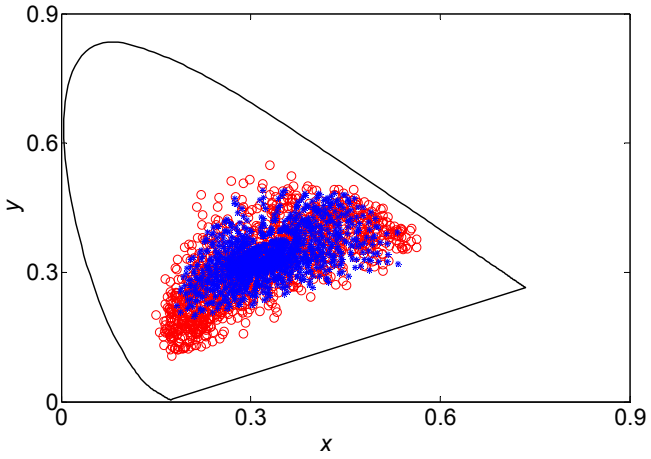

Figure 2: Chromaticity of Munsell (blue asterisks) samples and model-reflectance (red circles) samples.

Table 1 shows that in the Frequency domain, the two sets of reflectance have similar properties; both consist of band-limited functions. These results show that the reflectance spectra generated by the model have similar characteristics to the Munsell samples in terms of chromaticity and spectral frequency. All of the spectra generated by the model have reflectance spectra in the range 0-1.

Table 1: Proportion of spectral energy below a frequency limit for two data sets.

Band limit (cyc/nm)	**0.0050**	**0.0100**	**0.0150**	**0.0200**	
Munsell reflectance	0.9759	0.9916	0.9945	0.9962	lower quartile
	0.9968	0.9986	0.9992	0.9994	median
	0.9999	1.0000	1.0000	1.0000	upper quartile
Model reflectance	0.9919	0.9957	0.9971	0.9980	lower quartile
	0.9987	0.9993	0.9996	0.9997	median
	1.0000	1.0000	1.0000	1.0000	upper quartile

However, we also found some differences between the two data sets. The average reflectance of both data sets in Figure 3 shows that the Munsell data set has a property that represents higher values at the far end of the spectrum than the near end of the spectrum, while the model reflectance data we generated doesn't have this characteristic; the mean reflectance of the model is virtually a flat curve (resulting from the random choice of the parameters of the Gaussian distribution). The shape of the mean reflectance of the Munsell set may indicate that for the Munsell samples there are more absorption bands occurring in the short-wave region of the visible spectrum than in the long-wave region.

Table 2 shows the reconstruction error when using the model to represent existing reflectance curves. Representations of a set of 100 reflectance spectra from the same 1269 Munsell data were evaluated and compared with representations using basis functions. The accuracy of representation in either spectral (RMS) or colorimetric (ΔE) terms is similar for the physical model and a linear model using 7 basis functions. As expected, however, the linear model is more efficient (the physical model requires up to 15 parameters). Nevertheless, one advantage of the physical model is that all of the spectra are guaranteed to be physically realisable in the range 0-1 whereas this is not the case for the

linear model. Further work is underway to use fewer, but skewed, Gaussian functions in the physical model.

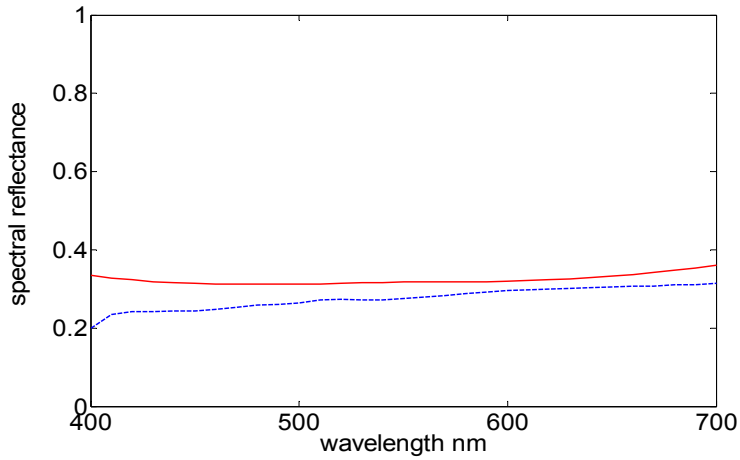

Figure 3: Average reflectance of Munsell data (dashed line) set and the model reflectance (solid line).

Table 2: Comparison of reconstruction errors of 100 Munsell reflectance using physical and linear models in root-mean- square (RMS) and CIELAB ΔE.

	Fitting error	Mean	Max	Min
Absorption model	RMS	0.0058	0.0279	0.000647
	ΔE	0.4100	3.0500	0.0300
4 basis functions	RMS	0.0123	0.062	0.0620
	ΔE	1.6500	12.4200	0.1900
5 basis functions	RMS	0.0093	0.038	0.0380
	ΔE	0.8700	5.5200	0.0400
6 basis functions	RMS	0.0072	0.0278	0.0278
	ΔE	0.3300	3.6100	0.0300
7 basis functions	RMS	0.0054	0.0159	0.0159
	ΔE	0.1700	0.6500	0.0100

References

1. L.T. Maloney, "Evaluation of linear models of surface spectral reflectance with small numbers of parameters," *Journal of the Optical Society of America A*, **3** (10), pp. 1673-1683, 1986.
2. D.Y Tzeng, R.S. Berns, "A review of principal component analysis and its applications to color technology," *Color Research and Application*, **30** (2), pp. 84-98, 2005.
3. K. Nassau, *The Physics and Chemistry of Color: The Fifteen Causes of Color*, John Wiley & Sons, 1983.
4. J.M. Sunshine, C.M. Pieters, and S.F. Pratt, "Deconvolution of mineral absorption bands: An improved approach*," Journal of Geophysical Research*, **95** (B5), pp. 6955-6966, 1990.
5. J.P.S Parkkinen, J. Hallikainen and T. Jaaskelainen, "Characteristic spectra of munsell colors," *Journal of the Optical Society of America A*, **6** (2), pp. 318-322, 1989.
6. M. De La Maza and D. Yuret, "Dynamic Hill Climbing," *AI Expert*, **9** (3), pp. 26-31, 1994.